ISSN 1069-3513, Izvestiya, Physics of the Solid Earth, 2013, Vol. 49, No. 6, pp. 786–795. © Pleiades Publishing, Ltd., 2013.
Original Russian Text © Yu.F. Kopnichev, I.N. Sokolova, K.N. Sokolov, 2013, published in Fizika Zemli, 2013, No. 6, pp. 39–48.

# Spatio-Temporal Variations in the Structure of the Attenuation Field of the *S*-Wave in the Region of Nevada Nuclear Test Site

**Yu. F. Kopnichev[a], I. N. Sokolova[b], and K. N. Sokolov[c]**

[a] *Schmidt Institute of Physics of the Earth, Russian Academy of Sciences, ul. Bol'shaya Gruzinskaya 10, Moscow, 123995 Russia*
*e-mail: yufk@kndc.kz*

[b] *Institute of Geophysical Research, National Nuclear Center, Republic of Kazakhstan, ul. Chaikinoi 4, Almaty, Republic of Kazakhstan*

[c] *St. Petersburg State Technical University, Politekhnicheskaya ul. 29, St. Petersburg, 195251 Russia*
*e-mail: sokolova@kndc.kz*

Received August 13, 2012; in final form, March 13, 2013

**Abstract**—The characteristics of the attenuation field of short-period shear waves in the region of Nevada nuclear test site (NNTS) are studied. The seismograms of underground nuclear explosions (UNEs) and earthquakes recorded by three seismic stations in 1975–2012 at the epicentral distances of up to 1000 km are processed by the methods based on the analysis of the amplitude ratios of *Sn* to *Pn* and *Lg* to *Pg* waves, as well as the *S*-coda envelopes for close events. It is shown that the structure of the attenuation field in the Earth's crust and upper mantle in the NNTS region experienced significant temporal variations during the interval of nuclear operations. The strongest variations were associated with UNEs conducted in the Pahute Mesa area, which held about two-thirds of the most intense explosions. Our data indicate that temporal variations in the structure of the attenuation field are related to the migration of deep fluids. A comparison of the general characteristics of the attenuation field in the regions of the three large nuclear test sites is presented.

**DOI:** 10.1134/S1069351313060086

## INTRODUCTION

In (Kopnichev and Sokolova, 2001), the spatiotemporal variations in the attenuation field of *S* waves in the Earth's crust and upper mantle were studied in the region of the Semipalatinsk nuclear test site (SNTS). The strongest variations in attenuation were observed in the Balapan area, which held the strongest UNEs (Mikhailov et al., 1996). Time variations in the attenuation field have also been identified in the region of the Lop Nor nuclear test site (LNTS) in China (Kopnichev and Sokolova, 2012a; 2012b), where the number of the underground shots was by an order of magnitude lower than at SNTS (Fisk, 2002). In the present work, we study spatiotemporal variations in the *S*-wave attenuation field in the region of the world's largest nuclear test site in Nevada, where the highest number of nuclear tests have taken place (more than 800 (*United*..., 2000; Adushkin and Spivak, 2007)).

## THE GEOLOGICAL AND GEOPHYSICAL OUTLINE OF THE REGION

NNTS is located in the southern part of the vast rift zone in western United States (the Basin and Range Province, Fig. 1). The rift zone was formed as a result of sublatitudinal tectonic extension of the lithosphere, which started about 17 Ma ago (Sinnock, 1982). The topography of the rift zone is dominated by the sequence of parallel ranges and basins forming a "keyboard" block system. The crustal thickness in the region is about 35 km (Kumar et al., 2012). Just as the rift zone overall, the territory of NNTS is marked by a high heat flux (Grachev, 1977).

The northwestern corner of NNTS comprises the Pahute Mesa area, which is mainly composed of volcanics dominated by tuffs (Sinnock, 1982) (Fig. 1a). This area is topographically uplifted up to 600 m above the neighboring planes. The northeastern part of NNTS is occupied by the Yucca Flat desert drainage basin largely composed of Quaternary sedimentary rocks with a thickness of up to 600 m. In the east, the Yucca Flat area is constrained by a narrow Halfpint Range. The ancient volcanic caldera of Timber Mountain is located south of Pahute Mesa. The southernmost part of the test site comprises the Jackass Flats and Frenchman Flat basins.

During the period from 1962 to 1992, more than 800 UNEs with a maximal announced yield of 1300 kilotons were shot in the NNTS (*United*..., 2000). The bulk of the UNEs, including the largest explosions with a yield of above 100 kilotons, were detonated in the Pahute Mesa and Yucca Flat areas. Most of the highest yielding tests up to 500–1000 kilotons

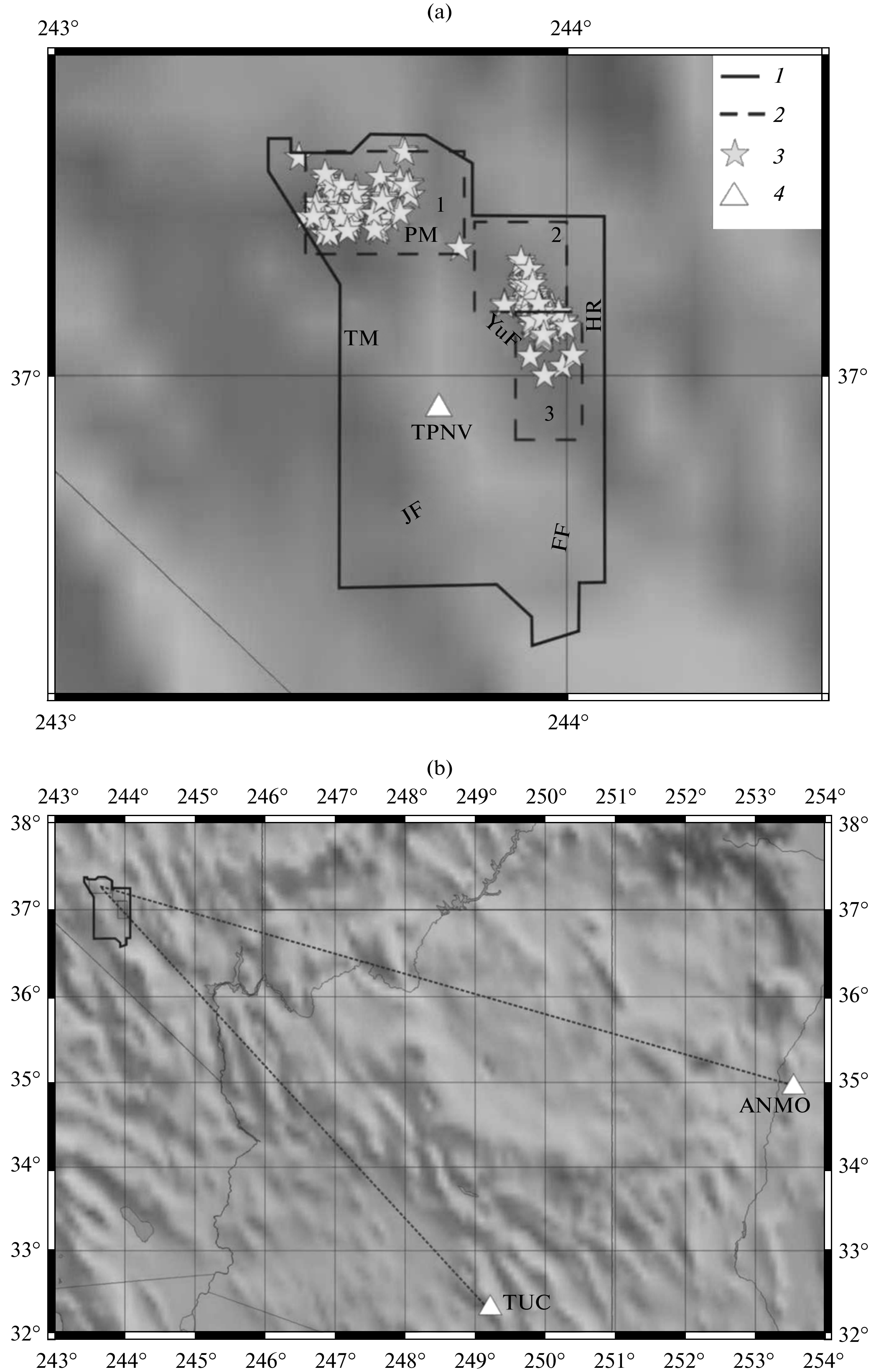


**Fig. 1.** The map of the region of study (a): (*1*) the configuration of NNTS; (*2*) the positions of the considered sites; (*3*) the epicenters of the strongest explosions ($Y > 20$ kilotons); (*4*) the seismic station. The tectonic structures: PM, Pahute Mesa; TM, Timber Mountain; HR, Halfpint Range; YuF, Yucca Flat; JF, Jackass Flats, and FF, Frenchmen Flat areas; (b) the layout of seismic stations ANMO and TUC relative to NNTS.

were conducted in 1975–1976. After 1976, the maximal yield of the shots was 150 kilotons.

At present, the NNTS region is characterized by weak seismic activity. After termination of nuclear operations, the strongest earthquake occurred here in 1999 and had magnitude $M = 4.5$. Since 2000, seismic events with $M > 3.6$ have not been detected in the region.

## THE DATA AND PROCESSING

We analyzed the records of UNEs and earthquakes from the ANMO and TUC digital seismic stations for the intervals of 1975–2002 and 1992–2011, respectively (Figs. 1a, 1b, and 2). The epicentral distances for these stations varied within ~800–940 and 620–940 km, respectively. Overall, more than 180 records of UNEs and 50 records of earthquakes were considered.

Besides, we have processed ten seismograms of local earthquakes and one chemical explosion recorded by the TPNV digital station (Fig. 1a) in 1993–2012 at the epicentral distances up to 40 km.

In the analysis of seismograms from the ANMO and TUC stations at epicentral distances within 1000 km, we calculated the amplitude ratios for the *Lg* to *Pg* waves and *Sn* to *Pn* waves. For brevity, we denote *lg*(*ALg*/*APg*) and *lg*(*ASn*/*APn*) by *Lg*/*Pg* and *Sn*/*Pn*, respectively. The *Lg* and *Pg* waves propagate in the crust, and their amplitude ratio describes the attenuation of *S*-waves along the entire path from the source to the station (Kopnichev, 1985). The *Sn* and *Pn* waves penetrate below the Moho, and their *Sn*/*Pn* ratio, with other conditions being equal, reflects the degree of attenuation of the *S*-waves in the top layers of the mantle in the area of the source (Molnar and Oliver, 1969; Kopnichev and Arakelyan, 1988; Kopnichev and Sokolova, 2010; 2011).

The interpretation of the records of local earthquakes and chemical explosion was based on the analysis of the characteristics of short-period *S*-coda. It was previously established that at a frequency of about 1 Hz, a coda is mainly formed by the shear waves reflected from numerous subhorizontal boundaries in the Earth's crust and upper mantle (Kopnichev, 1985; Aptikaeva and Kopnichev, 1993). With this scenario of coda formation, the segments of the relatively fast and slow decay of coda amplitudes are associated with the penetration of *S* waves into the layers characterized by high and low attenuation, respectively. The depths of these layers are determined with the assumption that a coda is formed by the UNEs reflected waves. The attenuation in our study is evaluated in terms of the effective $Q$ factor, $Q_s$, which was calculated from the decay of coda amplitudes according to the formula $A(t) \sim \exp(-\pi t/Q_s T)/t$, where $T$ is the period of oscillations, and time $t$ is measured from the onset of wave radiation in the source (Kopnichev, 1985).

It was previously shown that voids and fractured zones, as well as the changes in the ground water dynamics due to UNEs (Adushkin and Spivak, 1993), do not present a serious obstacle for studying the attenuation field at sufficiently large depths by the described methods (Kopnichev and Sokolova, 2001).

The seismogram processing included narrow-band filtering, which eliminated the effects associated with the differences in the source radiation spectra for different events, and the frequency dependence of the $Q$ factor (Kopnichev, 1985; Aptikaeva and Kopnichev, 1993). We used the filter with a central frequency of 1.25 Hz and 2/3 octave bandwidth at a level of 0.7, which is similar to the corresponding channel of the frequency-selective seismic station (Kopnichev, 1985).

## THE ANALYSIS OF THE DATA

We subdivided the part of the NNTS territory that contains the epicenters of the explosions analyzed in our study into three sites (Fig. 1). The first site largely corresponds to the Pahute Mesa area, and the second and third sites, to the Yucca Flat region. These sites held all the sufficiently large explosions with the minimal announced yield $P$ ranging within 20–150 kilotons (*United...*, 2000). At the same time, the number of the largest UNEs ($Y > 100$ kilotons) detonated within the first site was severalfold larger than within either of the two other sites. From Fig. 1 it follows that the paths from site 1 to the ANMO station mostly pass through site 2, and the paths to TUC station partly intersect sites 2 and 3.

### *The Analysis of the Records of UNEs and Earthquakes from the ANMO and TUC Stations*

The examples of the seismograms from the ANMO station, which recorded the explosions in the three selected NNTS sites, are presented in Fig. 3. The common features observed in all the records are the high *Sn*/*Pn* and rather low *Lg*/*Pg* ratios.

Figures 4–9 show the time behavior of the mean *Sn*/*Pn* and *Lg*/*Pg* for UNEs. From Fig. 4 it follows that after the interval of very low *Sn*/*Pn* in 1975–1978, this parameter sharply increased from 0.41 to 0.61 in 1979–1982, far in excess of the confidence interval at the level of 0.9 corresponding to the data for 1975–1978. This rise was followed by a gradual decline to 0.48 in 1989–1992. A similar pattern was also observed in the data for site 2 (Fig. 5), although with a much narrower span of the variations (within 0.52–0.62). At site 3, variations in *Sn*/*Pn* were insignificant (0.56–0.60); they did not exceed the confidence interval for the mean value estimated from the data for 1975–1978 (Fig. 6).

A strikingly different behavior is observed in the variations of *Lg*/*Pg*. Figure 7 shows that at site 1, this parameter abruptly dropped from –0.35 in 1983–1986 to –0.55 in 1975–1978, again far beyond the confidence interval corresponding to the data of 1975–

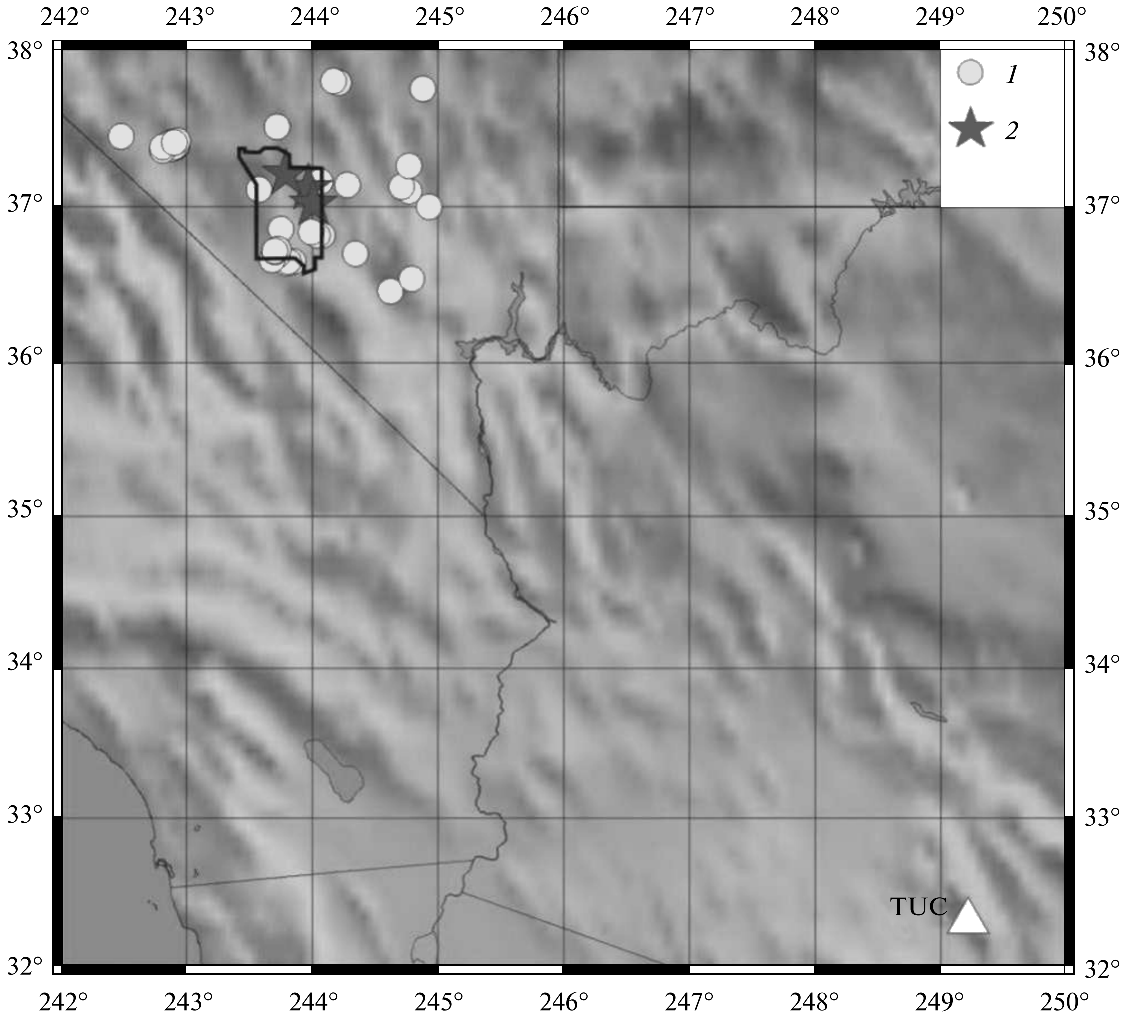


**Fig. 2.** The epicenters of the (*1*) earthquakes and (*2*) UNEs recorded by TUC station.

1978. After the drop, the mean *Lg*/*Pg* remained at approximately this level. At the same time, the *Lg*/*Pg* for site 2 monotonically increased from –0.35 to –0.15 during the considered time interval (Fig. 8). The variations in this parameter for site 3 were again the lowest, ranging between –0.34 in 1975–1978 and –0.46 in 1987–1992 (Fig. 9).

For comparison, Figs. 4 and 7 show the mean *Sn*/*Pn* and *Lg*/*Pg* for the earthquakes that occurred in 1976 within site 1. These values are significantly higher (by 0.4–0.5 log units) than for UNEs in 1975–1978.

The seismograms at the TUC station were used for analyzing the waveforms of UNEs and earthquakes that took place in 1992–2011. From Figs. 10 and 11 it follows that in the northern part of NNTS, which includes the three sites considered here, the mean *Sn*/*Pn* for the earthquakes are appreciably higher (by 0.17 log units) and the mean *Lg*/*Pg* are lower (by 0.25 log units) than in the southernmost part of NNTS, where UNEs were almost not conducted. Comparing the results for the earthquakes with the data for UNEs conducted in 1992 at sites 1 and 2, we see that the mean *Sn*/*Pn* and *Lg*/*Pg* for the earthquakes whose epicenters were located in the northern segment of NNTS are higher than for the explosions by 0.20 and 0.15 log units, respectively.

Figure 12 illustrates the dependence of *Sn*/*Pn* on the distance estimated from the records by TUC station for the profile cutting NNTS. From the graph it follows that the mean *Sn*/*Pn* for the earthquake epicenters located in the NNTS region are dramatically higher than in the areas east and west of the nuclear test site.

### *The Analysis of the Seismograms of the Earthquakes and Chemical Explosions from TPNV Station*

Figure 13 shows the common *S*-coda envelopes for the records of the local earthquakes and one chemical explosion from TPNV station. This station is located 25 km south of the southern boundary of site 1. The graphs for the epicenters located within site 1 contain

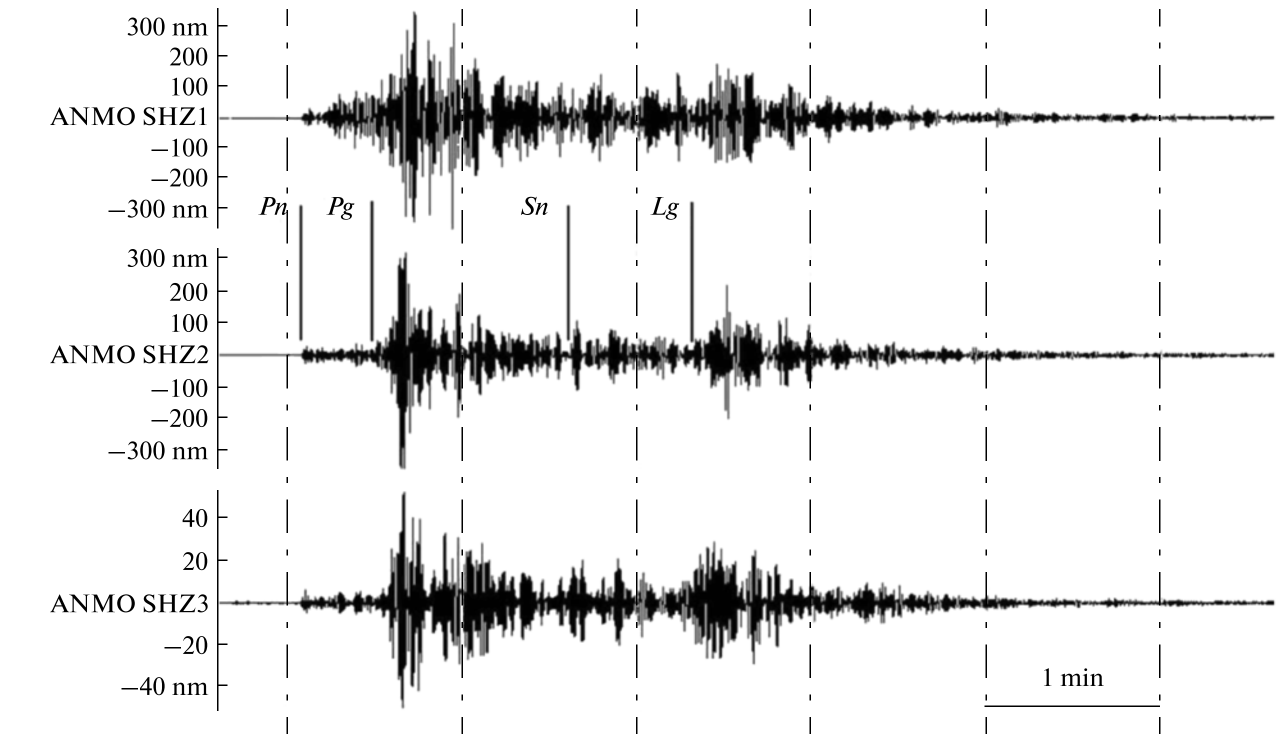


**Fig. 3.** The example of the seismograms of UNEs recorded by ANMO station. The upper path corresponds to site 1 (15:30:00 on December 17, 1978); the middle path corresponds to site 2 (20:00:00 on April 16, 1980); the upper path corresponds to site 2 (15:20:00 on December 10, 1982). The arrows mark the arrivals of the wave groups considered.

the interval where the attenuation is very weak ($t$ = 19–47 s), which is followed by quite rapid decay in the interval $t$ = 47–64 s. For the epicenters located immediately south of site 1, the envelopes have a gently sloping interval at $t$ = 12–19 s, after which the amplitudes sharply decay at $t$ = 19–43 s. For the epicenters located even farther south, 50–55 km of the southern boundary of site 1, the envelopes have the interval of sharply attenuating amplitudes at $t$ = 17–40 s.

Figure 14 shows the cross sections of the attenuation field along the submeridional profile. The depth of the boundaries is determined within an accuracy of ~5 km in the lower crust and ~10 km in the upper mantle. It can be seen that for site 1, in the top portion of the mantle, the attenuation is very low ($Qs$ > 1000) in the depth interval of ~35–100 km. The $Q$-factor sharply drops to $Qs$ ~ 70 in the interval of ~100–135 km. After this, attenuation decreases again ($Qs$ ~ 200) at depth $h$ ~ 135–180 km. South of site 1, we observe extremely low attenuation ($Qs$ > 2000) in the lower crust at $h$ ~ 20–35 km and relatively high attenuation in the upper mantle ($h$ 35–130 km, $Qs$ = 80). Deeper in the mantle there is a relatively thin layer with a thickness of about 20 km, where the attenuation is very low ($Qs$ > 2000), below which the $Q$-factor again abruptly drops to $Qs$ ~ 180.

For the epicenters located south within ~50 km of the boundary of site 1, high attenuation is observed in the depth interval of ~30–80 km, below which the $Q$ factor noticeably increases: in the depth intervals of ~80–115 and 155–180 km, $Qs$ = 250 and 140, respectively.

From Fig. 14 it follows that in the upper layers of the mantle up to a depth of ~100 km beneath site 1, attenuation of the $S$-waves is far lower than south of this site.

## DISCUSSION

Our results indicate that during the period of nuclear test operations, the attenuation field of $S$-waves in the region of NNTS experienced significant variations. These variations can only be associated with the migration of the deep fluids (the ascent of the partially molten material, which also contributes to the high attenuation of the $S$-waves, can certainly be ruled out since the viscosity of the melt is by many orders of magnitude higher than the viscosity of the fluids).

The most favorable conditions for the migration of deep fluids exist in the lower crust, which is typically characterized by quite high fluid content, high electric conductivity (Vanyan and Haindman, 1996; Bielinski et al., 2003), and high attenuation of shear waves (Bakirov, 2006) in the tectonically active regions. Besides, narrow fluid-saturated zones, which can breach almost the entire lithosphere and are typically related to the deep faults (Berdichevskii et al., 1996;

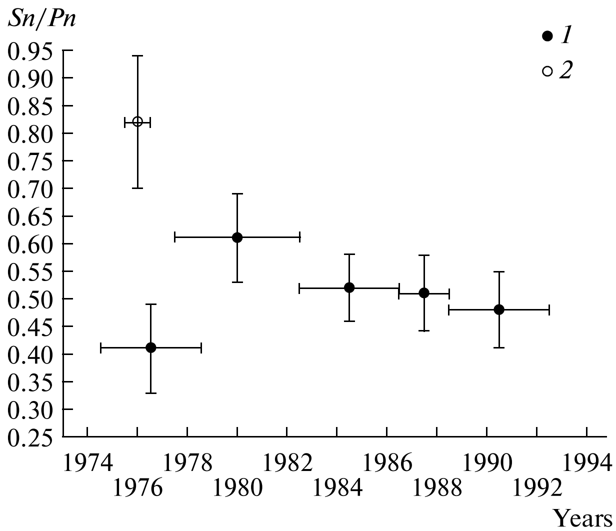


**Fig. 4.** The time dependence of mean *Sn/Pn* for (*1*) UNEs and (*2*) earthquakes that occurred within site 1. The confidence intervals at a level of 0.9 and the intervals of data averaging are shown here and in Figs. 5–9, the records from ANMO are used.

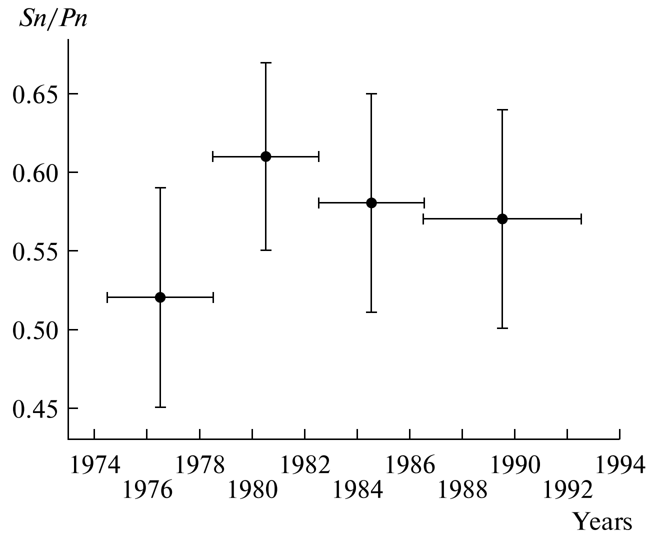


**Fig. 5.** The time dependence of the mean *Sn/Pn* for (*1*) UNEs and (*2*) earthquakes that occurred within site 2. The notations are the same as in Fig. 4.

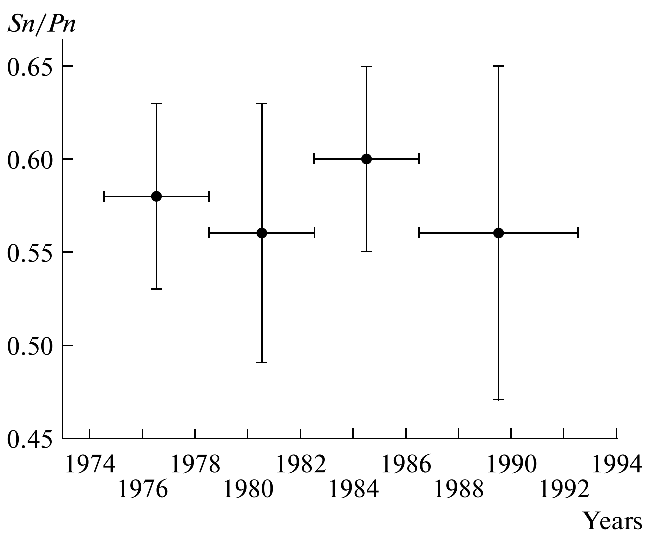


**Fig. 6.** The time dependence of the mean *Sn/Pn* for UNEs within site 3. The notations are the same as in Fig. 4.

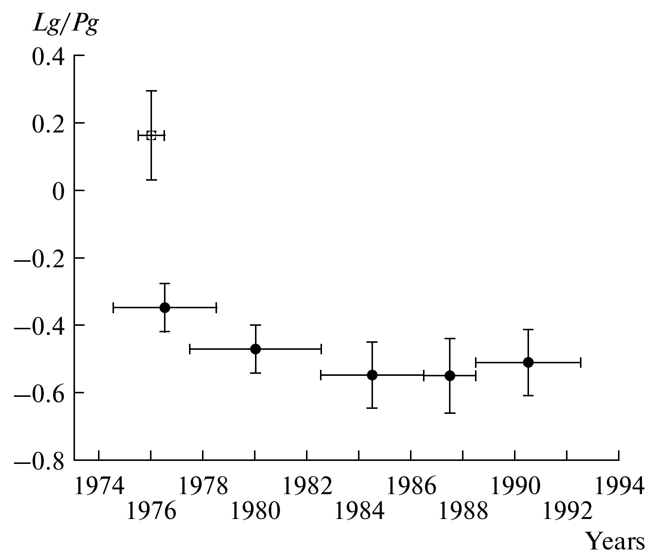


**Fig. 7.** The time dependence of the mean *Lg/Pg* for UNEs within site 1. The notations are the same as in Fig. 4.

Bakirov, 2006), are revealed in these regions. These zones may serve as the pathways for the fluids to rise from the upper mantle to the Earth's crust (Husen and Kissling, 2001; Kopnichev and Sokolova, 2003; Kopnichev, Gordienko, and Sokolova, 2009).

The rise of the fluids to the lower crust and their horizontal migration are probably accounted for by the long intensive anthropogenic impact on the geological environment, which resulted from a unique series of UNEs conducted in the NNTS. Vibration leads to the increase in the permeability of the rocks even in the model experiments (Barabanov et al., 1987); and a fortiori this could be expected at sufficiently large depths in the crust and upper mantle, where the Archimedes force tends to push the fluids to the surface (Gold and Soter, 1984/1985).

The migration distance of seismic rays in the lower crust for the raypaths of the waves forming the *Sn*- and

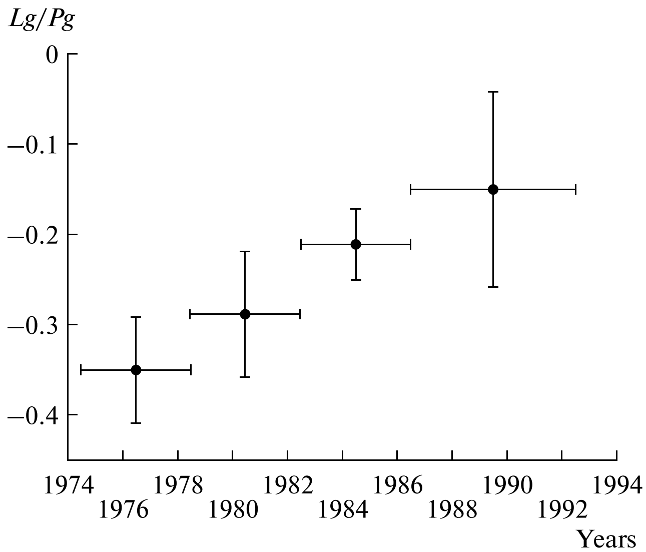


**Fig. 8.** The time dependence of the mean *Lg/Pg* for UNEs within site 2. The notations are the same as in Fig. 4.

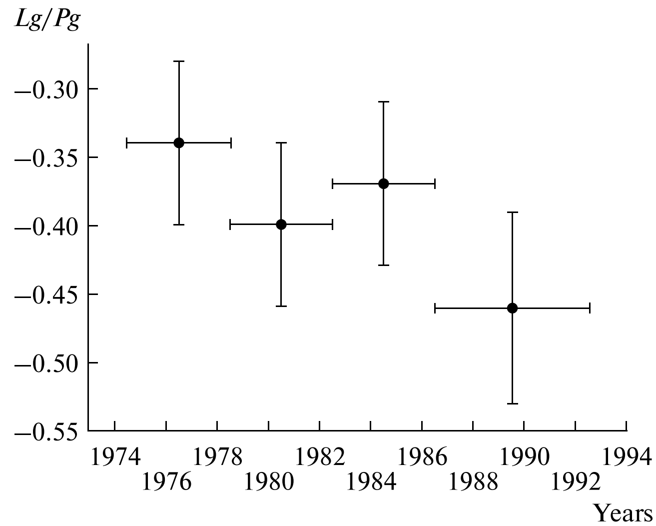


**Fig. 9.** The time dependence of the mean *Lg/Pg* for UNEs within site 3. The notations are the same as in Fig. 4.

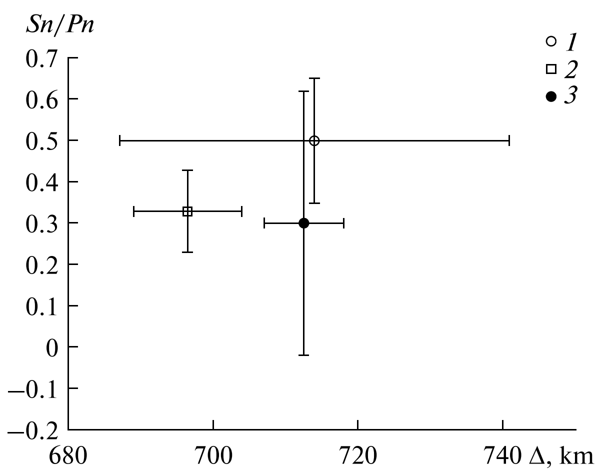


**Fig. 10.** The mean values of *Sn/Pn* for the earthquakes (*1*) in the north and (*2*) in the south of NNTS; (*3*) the same for UNEs. The data from TUC station are used.

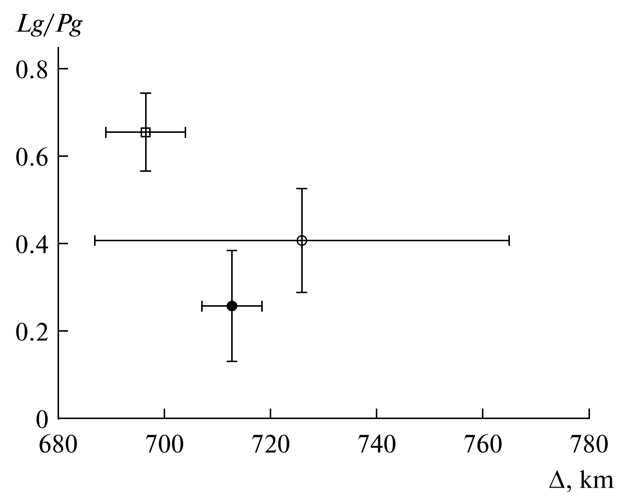


**Fig. 11.** The mean values of *Lg/Pg*. The notations are the same as in Fig. 10. TUC station.

*Lg*-group can be tentatively estimated in the following way. We consider the first-approximation two-layer model of the medium, in which the crust has a thickness of 35 km, and the *S* velocities in the crust and upper mantle are 3.5 and 4.6 km/s, respectively. In this case, the critical angle of incidence $i_{np}$ on the boundary *M*, which demarcates the raypaths forming the groups *Sn* and *Lg*, is ~49.5°. With this angle, the migration distance in the lower crust at a depth of 20–35 km is ~23–41 km. With a smaller migration distance, the waves escape into the upper mantle (with the formation of the *Sn* wave), while with a larger migration distance, the waves are captured by the crustal waveguide (and the *Lg*-group is formed) (Kopnichev, 1985; Kopnichev and Arakelyan, 1988).

From Figs. 4–6 it follows that the strongest variations in *Sn/Pn* correspond to site 1, which held 2/3 of the largest shots with a yield of more than 100 kilotons. The seismic paths from site 1 to the ANMO station pass through site 2, therefore the variations in this parameter can be associated with the changes in the structure of the attenuation field within both sites. The sharp growth in *Sn/Pn* for detonations in site 1 and the weaker increase in this parameter for the explosions at

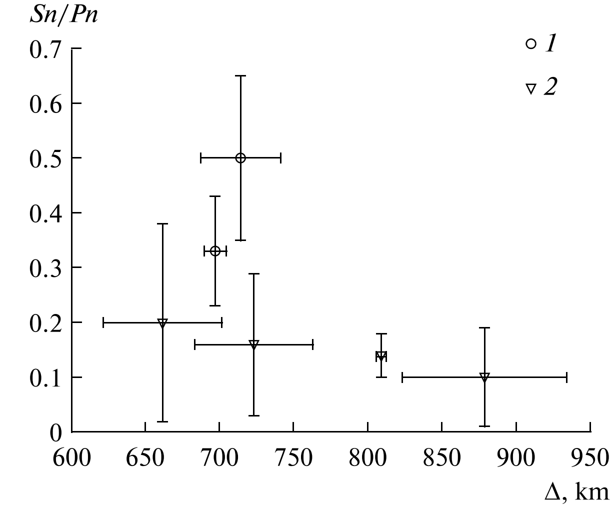


**Fig. 12.** The dependence of the mean values of *Sn/Pn* on the epicentral distance for the earthquakes (*1*) in the NNTS region and (*2*) close to NNTS. TUC station.

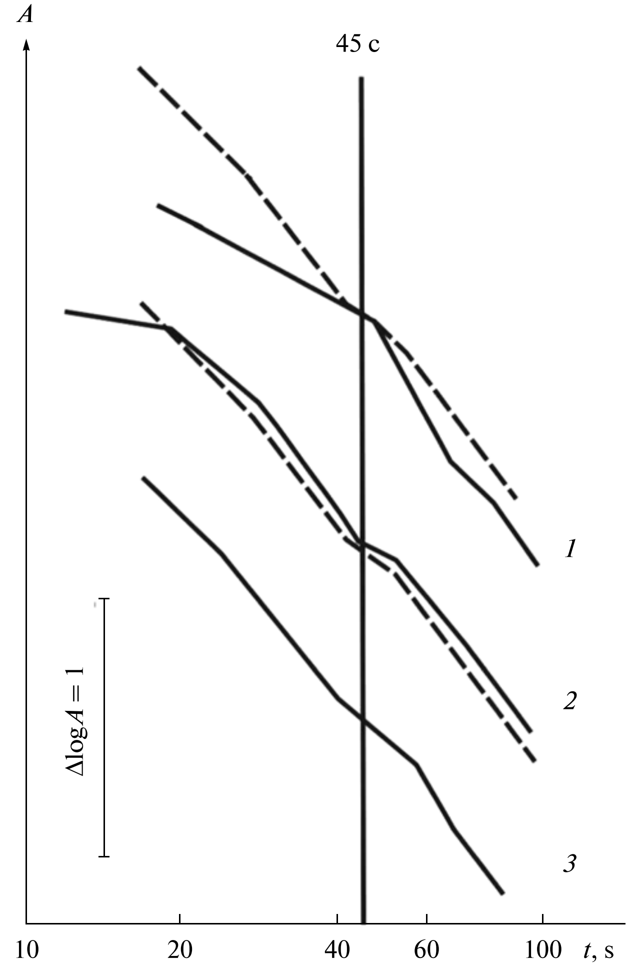


**Fig. 13.** The common *S*-coda envelopes for the earthquakes in the NNTS region: (*1*) the epicenters at site 1; (*2*) and (*3*) at a distance of about 5–10 and 50–55 km from the southern boundary of site 1. The dashed line is the envelope for the southernmost part of the region. TPNV station.

site 2 in 1979–1982 are correlated to the drop in the *Lg/Pg* parameter for the shots at site 1. This effect is probably due to the ascent of the fluids from the upper mantle to the lower crust at both sites and in the area located east-southeast of site 2. This interpretation agrees with the extremely low attenuation of the *S*-waves in the depth interval of 35–100 km in the area of site 1, revealed from the records of local events. Furthermore, this is also supported by the sharp increase in *Sn/Pn* derived from the records of the earthquakes in the NNTS region for the profile cutting the test site (TUC station, Fig. 12). Remarkably, the strongest variation in *Sn/Pn* is observed starting from 1978, only one year after the interval of the strongest energy release at the test site, which occurred in 1975–1976.

The gradual decline in *Sn/Pn* for the shots at sites 1 and 2 after 1982 is most likely to be associated with the new episode of the rise of fluids to the upper mantle. Besides, the growth in the mean *Lg/Pg* for UNEs shot at site 2 in 1979–1992 can probably indicate the additional migration of the fluids to this site across the lower crust from the Halfpint Range region, where the waves forming the *Lg* group start to penetrate into the lower crust.

For the shots conducted in site 3, which held the fewest largest explosions among the sites considered, the value of *Sn/Pn* has barely changed during the last 17 years, while the value of *Lg/Pg* noticeably dropped as late as 1987–1992. This can indicate that the fluids did not well up to the lower crust in the area located east-southeast of this site, and their migration across the lower crust to this region started relatively late, at the end of the 1980s.

The analysis of Figs. 10 and 11 shows that the difference between the mean values of *Sn/Pn* and *Lg/Pg* for the earthquakes recorded in 1992–2011 and UNE in 1992 (according to the data from TUC station) is far smaller than for such events recorded in 1976 and 1975–1978 (according to the data from ANMO station), respectively. In our opinion, this could be associated with the ongoing rise of the fluids to the upper mantle and crust after termination of a long series of UNEs. The similar effect was previously established for the Lop Nor region (Kopnichev and Sokolova, 2012b).

We have compared the general characteristics of the attenuation field in the regions of three nuclear test sites. It was shown previously that at SNTS, which is located within the tectonically stable Kazakh Platform, the strong attenuation of the *S*-waves at the beginning of the 2000s was observed in the crust and upper mantle below the Balapan site, which is cut by two regional faults and where the largest UNEs with a yield up to 165 kilotons were conducted (Kiopnichev and Sokolova, 2001). LNTS is located in the seismi-

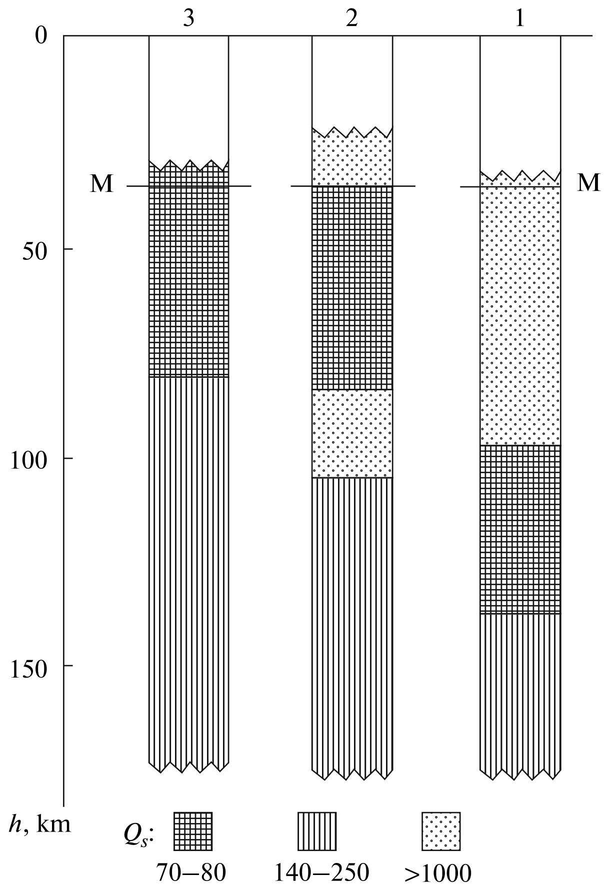


**Fig. 14.** The cross sections of the *S*-wave attenuation field in the region of NNTS. The numbers correspond to the envelopes in Fig. 13. The hatches correspond to the different intervals of the variations in the $Q_S$ parameter.

cally active East Tien Shan region, where the earthquakes with $M > 7$ are documented (Kopnichev and Sokolova, 2012a). According to our data, during the interval of nuclear tests in 1969 to 1996, which includes 22 explosions with a maximum yield of 600–700 kilotons, the attenuation in this area significantly increased in the upper mantle and remained relatively low in the crust (Kopnichev and Sokolova, 2008; 2012b). The most reasonable interpretation of these effects associates them with the difference in the permeability of the rocks and total energy released by nuclear operations at these three sites. Within NNTS, where the permeability of the lithosphere and the energy release are highest, the top portion of the mantle has been drained to a considerable extent, and the fluid content in the crust has overall increased. In the region of SNTS, where the permeability of the lithosphere is lowest, but where close to 350 explosions were conducted, the processes of fluid migration were sufficiently intense only within the Balapan site, where they were concentrated in the depth interval from ~10 to 120 km (Kopnichev and Sokolova, 2001). In the region of LNTS, where the lithosphere has intermediate permeability but the energy release was lowest, the fluids were probably concentrated in the upper mantle and were not abundantly supplied to the Earth's crust.

Our data present new evidence that long-lasting intense anthropogenic impacts violate the equilibrium in the lithosphere up to quite deep horizons. The similar effects of fluid ascent from the upper mantle are observed after the large tectonic earthquakes (Husen and Kissling, 2001; Kopnichev and Sokolova, 2003; Kopnichev, Gordienko, and Sokolova, 2009). In both cases, these processes eventually reduce the potential energy of the Earth.

## ACKNOWLEDGMENTS

We are grateful to Incorporated Research Institutions for Seismology Data Management Center (IRIS DMC) for providing the data from the digital seismic stations.

## REFERENCES

Adushkin, V.V. and Spivak, A.A., Changes in the groundwater level due to underground nuclear explosions, *Byull. TsOIAE*, 1993, no. 9, pp. 38–43.

Adushkin, V.V. and Spivak, A.A., *Podzemnye vzryvy* (Underground Explosions), Moscow: Nauka, 2007.

Aptikaeva, O.I. and Kopnichev, Yu.F., Space-time variations of the coda wave envelopes of local earthquakes in the region of Central Asia, *J. Earthq. Predict. Res.*, 1993, vol. 2, no. 4, pp. 497–514.

Bakirov, A.B., Ed., *Zemnaya kora i verkhnyaya mantiya Tyan'-Shanya v svyazi s geodinamikoi i seismichnost'yu* (Earth's Crust and Upper Mantle of Tien Shan in Relation to Geodynamics and Seismicity), Bishkek: Ilim, 2006.

Barabanov, V.L., Grinevskii, A.O., Kissin, I.G., and Nikolaev, A.V., On some effects of seismic vibration in a fluid-saturated medium: comparison with the effects of the strong remote earthquakes, *Dokl. Ross. Akad. Nauk*, 1987, vol. 297, no. 1, pp. 53–56.

Berdichevsky, M.N., Borisova, V.P., Golubtsova, N.S., Ingerov, A.I., Konovalov, Yu.F., Kulikov, A.V., Solodilov, L.N., Chernyavskii, G.A., and Shpak, I.P., Interpretation of magnetotelluric soundings in the Lesser Caucasus, *Izv., Phys. Solid Earth*, 1996, vol. 32, no. 4, pp. 365–370.

Bielinski, R., Park, S., Rybin, A., Batalev, V., Yun, Sh., and Sears, C., Lithospheric heterogeneity in the Kyrgyz Tien Shan imaged by magnitotelluric stidies, *Geophys. Rev. Lett.*, 2003, vol. 30, no. 15. doi: 10.1029/2003GL017455

Fisk, M., Accurate locations of nuclear explosions at the Lop Nor test site using alignment of seismograms and ICONOS satellite imagery, *Bull. Seismol. Soc. Amer.*, 2002, vol. 92, no. 8, pp. 2911–2525.

Gold, T. and Soter, S., Fluid ascent through the solid lithosphere and its relation to earthquakes, *Pure Appl. Geophys.*, 1984/1985, vol. 122, pp. 492–530.

Grachev, A.F., *Riftovye zony Zemli* (Rift Zones of the Earth), Leningrad: Nedra, 1977.

Husen, S. and Kissling, E., Postseismic fluid flow after the large subduction earthquake of Antofagasta, Chile, *Geology*, 2001, vol. 29, no. 9, pp. 847–850.

Kopnichev, Yu.F., *Korotkoperiodnye seismicheskie volnovye polya* (Short-Period Seismic Wave Fields), Moscow: Nauka, 1985.

Kopnichev, Yu.F. and Arakelyan, A.R., On the nature of short-period seismic fields within a distance of 3000 km, *Vulkanol. Seismol.*, 1988, no. 4, pp. 77–92.

Kopnichev, Yu.F. and Sokolova, I.N., Space–time variations in the attenuation field structure of *S* Waves at the Semipalatinsk Test Site, *Izv., Phys. Solid Earth*, 2001, vol. 37, no. 11, pp. 928–941.

Kopnichev, Yu.F. and Sokolova, I.N., Spatiotemporal variations of the *S* wave attenuation field in the source zones of large earthquakes in the Tien Shan, *Izv., Phys. Solid Earth*, 2003, vol. 39, no. 7, pp. 568–579.

Kopnichev, Yu.F. and Sokolova, I.N., Shear wave attenuation field of heterogeneities in the Earth's crust and upper mantle in the Lop Nor Test Site area, *Dokl. Earth Sci.*, 2008, vol. 420, no. 2, pp. 649–652.

Kopnichev, Yu.F. and Sokolova, I.N., On the geodynamical processes in the regions of three nuclear test sites, *Vestnik NYaTs RK*, 2009, no. 3, pp. 48–54.

Kopnichev, Yu.F., Gordienko, D.D., and Sokolova, I.N., Space–time variations of the shear wave attenuation field in the upper mantle of seismic and low seismicity areas, *J. Volcanol. Seismol.*, 2009, vol. 3, no. 1, pp. 44–58.

Kopnichev, Yu.F. and Sokolova, I.N., Heterogeneities in the absorption field of short-period S-waves in the lithosphere of Tien Shan and Dzungaria with their relation to seismicity, *Dokl. Earth Sci.*, 2010, vol. 433, no. 6, pp. 1119–1123.

Kopnichev, Yu.F. and Sokolova, I.N., Heterogeneities of the field of short-period transverse wave absorption in the lithosphere of Central Asia and their relationship with seismicity, *Dokl. Earth Sci.*, 2011, vol. 437, no. 1, pp. 363–367.

Kopnichev, Yu.F. and Sokolova, I.N., Heterogeneities of the shear wave attenuation field in the lithosphere of East Tien Shan and their relationship with seismicity, *Dokl. Earth Sci.*, 2012a, vol. 442, no. 2, pp. 292–295.

Kopnichev, Yu.F. and Sokolova, I.N., Time variations in the *S* wave attenuation field in the regions of Lop Nor and Novaya Zemlya nuclear test sites, *Vestnik NYaTs RK*, 2012b, no. 2.

Kumar, P., Kind, R., Yuan, X., and Mechie, J., USArray receiver function images of the lithosphere-asthenosphere boundary, *Seismol. Res. Lett.*, 2012, vol. 83, no. 3, pp. 486–491.

Mikhailov, V.N., Ed., *Ispytaniya yadernogo oruzhiya i yadernye vzryvy v mirnykh tselyakh SSSR, 1949-1990* (Nuclear Weapon Tests and Peaceful Nuclear Explosions in the USSR, 1949–1990), Sarov: RFYaTs-VNIIEF, 1996.

Molnar, P. and Oliver, J., Lateral variation of attenuation in the upper mantle and discontinuities in the lithosphere, *J. Geophys. Res.*, 1969, vol. 74, pp. 2648–2682.

Sinnock, S., *Geology of the Nevada Test Site and Nearby Areas, Southern Nevada*, Sandia Report SAND82-2207, 1982.

*United States Nuclear Tests: July 1945 through September 1992*, Las Vegas: U.S. Department of Energy, Nevada Operations Office, December 2000.

Vanyan, L.L. and Hyndman, R.D., Nature of electrical conductivity of the Earth's crust, *Izv., Phys. Solid Earth*, 1996, vol. 32, no. 4, pp. 261–267.

*Translated by M. Nazarenko*